

Synthesis, Crystal Structure, Magnetic Properties and ^{57}Fe Mössbauer Spectroscopy of the New Trinuclear $[\text{Fe}_3(4\text{-(2'-hydroxyethyl)-1,2,4-triazole})_6(\text{H}_2\text{O})_6](\text{CF}_3\text{SO}_3)_6$ Spin Crossover Compound

Yann Garcia,^[a] Philippe Guionneau,^[b] Georges Bravic,^[b] Daniel Chasseau,^[b] Judith A. K. Howard,^[c] Olivier Kahn[†],^[b] Vadim Ksenofontov,^[a] Sergei Reiman,^[a] and Philipp Gütlich^{*[a]}

Dedicated to Professor Arndt Simon on the occasion of his 60th birthday

Keywords: Iron / Spin crossover / Trinuclear complex / Hydrogen bonds / Mössbauer spectroscopy

$[\text{Fe}_3(\text{hyetrz})_6(\text{H}_2\text{O})_6](\text{CF}_3\text{SO}_3)_6$ [hyetrz = 4-(2'-hydroxyethyl)-1,2,4-triazole] represents the first structurally characterized iron(II) spin crossover compound for which the structure has been solved above and below room temperature in both spin states. The compound crystallizes in the trigonal system, space group $R\bar{3}$, $a = 12.763(1)$ Å, $\beta = 67.144(1)^\circ$, $V = 1684.3(1)$ Å³, $Z = 6$ at 120 K. At 330 K the space group is retained and $a = 13.0183(3)$ Å, $\beta = 67.376(3)^\circ$, $V = 1805.8(1)$

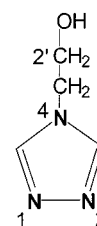
Å³. The molecular structure consists of trinuclear Fe^{II} entities linked together by an unprecedented three-dimensional network of hydrogen bonds. This compound shows a gradual spin crossover behavior centered around room temperature, which has been followed by temperature-dependent magnetic susceptibility measurements as well as by ^{57}Fe Mössbauer spectroscopy. The nature of the spin crossover behavior is discussed on the basis of the structural features.

Introduction

One of the appealing aspects of the phenomenon of spin crossover between high-spin (HS) and low-spin (LS) states resides in the occurrence of bistability, i.e. the possibility of observing two electronic states in a given range of external perturbation.^[1–3] In this respect, Fe^{II} spin crossover compounds have been widely investigated.^[4–7] For an assembly of spin crossover molecules governed by the thermodynamical regime, the perturbation may be caused by the temperature and then bistability leads to the occurrence of thermal hysteresis, which endows the system with a memory effect.^[1] A challenging field of research concerns the design of new Fe^{II} polynuclear spin crossover materials exhibiting strong inter-site interactions. A strategy towards obtaining such compounds consists of linking the active sites by chemical bridges to give extended or polymeric structures.^[8] Extensive research efforts have been directed towards Fe^{II} polymeric chain compounds containing 4-R-substituted derivatives of 1,2,4-triazole, because of the favorable characteristics of their spin crossover behavior.^[8–17] Such behavior

generally involves very abrupt transitions, as well as important thermal hysteresis effects accompanied by a pronounced thermochromic response, making them the compounds of choice for various applications in molecular electronics^[3,8,9,18] or as temperature sensors.^[8,14,17] So far, no crystal structure is available for these materials although several Cu^{II} structures have been solved.^[19–21]

Oligomers are generally used as model systems for the polymers because they are better defined from a crystallographic point of view and the physical properties can be easily correlated to the structural data. This is also the case for the Fe^{II} linear trinuclear compounds containing 4-R-substituted 1,2,4-triazole as ligands. Several crystal structures of these model compounds have been solved^[22–24] or have been studied by EXAFS spectroscopy.^[25] It was with this goal in mind that we decided to investigate the structure and magnetic properties of the new trinuclear compound of formula $[\text{Fe}_3(\text{hyetrz})_6(\text{H}_2\text{O})_6](\text{CF}_3\text{SO}_3)_6$ with hyetrz = 4-(2'-hydroxyethyl)-1,2,4-triazole (see Scheme 1).



Scheme 1. 4-(2'-hydroxyethyl)-1,2,4-triazole (hyetrz)

^[a] Institut für Anorganische Chemie und Analytische Chemie, Universität Mainz, Staudingerweg 9, 55099 Mainz, Germany
E-mail: P.guetlich@uni-mainz.de

^[b] Institut de Chimie de la Matière Condensée de Bordeaux, Laboratoire des Sciences Moléculaires, UPR CNRS No. 9048, 33608 Pessac, France

^[c] Durham Crystallography Group, Chemistry Department, Durham University, Durham, DH1 3LE, UK

This ligand was selected in order to increase the dimensionality through hydrogen bonding interactions. The compound shows a spin crossover behavior centered around room temperature. Its crystal structure has been solved in its LS and HS states. In addition, the dynamic character of the spin crossover behavior has been evidenced by ^{57}Fe Mössbauer spectroscopy.

Results

Description of the Structure of $[\text{Fe}_3(\text{hyetrz})_6(\text{H}_2\text{O})_6](\text{CF}_3\text{SO}_3)_6$

An atomic displacement ellipsoid plot of the molecule is represented in Figure 1 and relevant information on bond lengths and bond angles is given in Table 1.

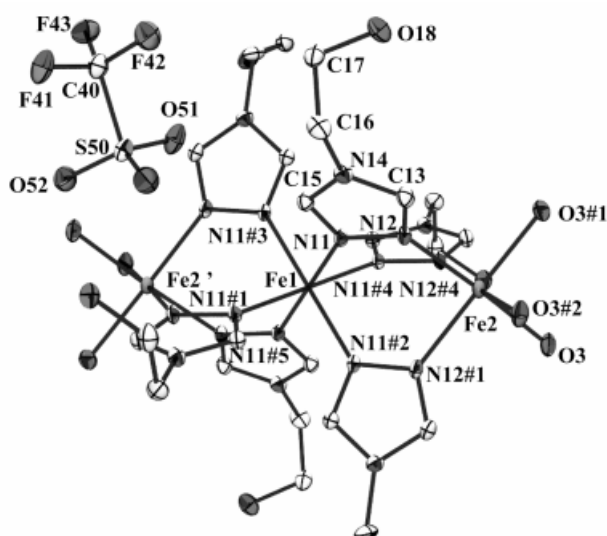


Figure 1. Atomic displacement ellipsoid view (50% probability) of the molecule of $[\text{Fe}_3(\text{hyetrz})_6(\text{H}_2\text{O})_6](\text{CF}_3\text{SO}_3)_6$ at 120 K. Hydrogen atoms have been omitted for clarity. Labeled atoms are generated by the following symmetry operations: #1 z, x, y ; #2 y, z, x ; #3 $-x, -y, -z$; #4 $-z, -x, -y$; #5 $-y, -z, -x$.

Table 1. Selected bond lengths [\AA] and angles [$^\circ$] of $[\text{Fe}_3(\text{hyetrz})_6(\text{H}_2\text{O})_6](\text{CF}_3\text{SO}_3)_6$ at 120 K and 330 K. Estimated standard deviations are given in parentheses

	$T = 120 \text{ K}$	$T = 330 \text{ K}$
Fe1–Fe2	3.7833(2)	3.8325(3)
Fe1–N11	2.003(1)	2.169(3)
Fe2–N12	2.161(2)	2.176(5)
Fe2–O3	2.124(2)	2.113(6)
N11–Fe1–N11#1 ^[a]	91.67(6)	89.2(2)
N11–Fe1–N11#4	88.33(6)	90.8(2)
N12–Fe2–N12#1	88.69(6)	92.1(2)
N12–Fe2–O3#1	88.57(6)	87.0(2)
N12–Fe2–O3#2	93.39(6)	91.2(2)
O3–Fe2–O3#1	89.44(6)	89.8(2)

^[a] Labeled atoms are generated by the following symmetry operations: #1 z, x, y ; #2 y, z, x ; #4 $-z, -x, -y$.

The title compound crystallizes in the trigonal space group $R\bar{3}$. The asymmetric unit contains one trifluoromethanesulfonate anion, one hyetrz ligand, one water molec-

ule, one iron(II) ion, which is labeled as Fe1 and located at the origin (occupancy factor of 1/6), and another iron(II) ion, Fe2, which lies at the special position $x = y = z$ (occupancy factor of 1/3). Thus, the crystalline unit contains one $[\text{Fe}_3(\text{hyetrz})_6(\text{H}_2\text{O})_6]^{6+}$ cation and six trifluoromethanesulfonate anions. The third iron(II) ion of the cation, labeled as Fe2', is the homolog of the Fe2 ion by the center of inversion on which the Fe1 ion lies. Three of the hyetrz ligands, which are homologous to one other by the 3-fold symmetry, act as bidentate ligands linking Fe1 to Fe2 through the nitrogen atoms N11 and N12. The three other hyetrz ligands, which are homologous to the former by the center of inversion, link Fe1 to Fe2'. Finally, the water molecules, linked to Fe2 and Fe2', complete the extremities of the trinuclear unit.

The Fe1 and Fe2 ions present octahedral surroundings. The environment of Fe1 is very regular as the six Fe1–N distances are all equal by symmetry. At 120 K, these bond lengths of 2.003(1) \AA correspond to the expected values for an Fe^{II} ion in the LS state.^[26] The adjacent N–Fe1–N bonds form an angle of 91.67(6) $^\circ$ when the nitrogen atoms are homologous by the 3-fold symmetry and an angle of 88.33(6) $^\circ$ when the nitrogen atoms are homologous by the center of symmetry. At 330 K, the Fe1–N distances are much longer [2.169(3) \AA] and correspond to a HS state.^[26] The N–Fe1–N angles are slightly different [89.2(2) $^\circ$ and 90.8(2) $^\circ$ respectively]. The environment of Fe2 is heterogeneous as this ion is bonded to three oxygen atoms and three nitrogen atoms, with only one atom of each species being crystallographically independent. The Fe2–N bond lengths are 2.161(2) \AA at 120 K [2.176(5) \AA at 330 K] and the Fe2–O bond lengths were found to be 2.124(2) \AA at 120 K [2.113(6) \AA at 330 K]. Thus, the Fe2 ions are in the HS state whatever the temperature and only the central iron(II) ion shows spin crossover behavior. The increase of the Fe1–N bond length from 120 K to 330 K is equal to 0.166 \AA , which is larger than the relatively weak increase (0.143 \AA) found for $[\text{Fe}_3(\text{etrz})_6(\text{H}_2\text{O})_6](\text{CF}_3\text{SO}_3)_6$.^[22] At 330 K, peripheral iron(II) octahedra become more compressed and regular. One can see this effect in a more pronounced way from the side of the oxygen atoms. This is a consequence of the increasing volume of the central iron(II) ion on going from the LS to the HS state. The Fe–Fe intramolecular distance significantly increases with temperature (see Table 1).

The least square planes through the triazole ligands form angles of 60 $^\circ$. This characteristic has already been observed for instance in the linear trinuclear compounds with the related ligand 4-ethyl-1,2,4-triazole (etrz), $[\text{M}_3^{\text{II}}(\text{etrz})_6(\text{H}_2\text{O})_6](\text{CF}_3\text{SO}_3)_6$ [$\text{M} = \text{Fe}$ (HS and LS),^[22] Mn ,^[27] Zn ^[28]], where a C_{32} symmetry is present. The N1,N2–1,2,4-triazole bridging ligands are all identical by symmetry and link the Fe^{II} ions with Fe–N–N bond angles of 127.59(8) $^\circ$ and 122.66(8) $^\circ$ in the LS state and of 125.7(2) $^\circ$ and 122.8(2) $^\circ$ in the HS state. All 1,2,4-triazole rings are planar; the deviation from the least-squares plane through the ring atoms is smaller than 0.002(1) \AA .

The crystal packing is built from the translation of the cation contained in the unit cell and thus, by symmetry, all

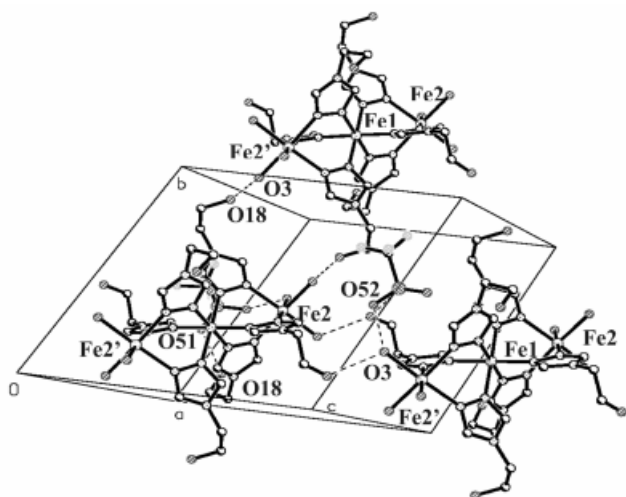


Figure 2. View of the intermolecular interactions between the trinuclear units of [Fe₃(hyetrz)₆(H₂O)₆](CF₃SO₃)₆ at 120 K

Table 2. Relevant interatomic distances (up to 3 Å) and angles of the hydrogen bonding interactions in [Fe₃(hyetrz)₆(H₂O)₆](CF₃SO₃)₆. Estimated standard deviations are given in parentheses

D—H...A	D—H	H...A	D...A	D—H...A
120 K				
O3—H31O18 (−z, −x, −1 − y)	0.81(3)	1.89(3)	2.700(2)	176(3)
O3—H32O52#3 ^[a]	0.83(3)	2.01(3)	2.829(2)	171(3)
O18—H181O51#5	0.78(3)	1.95(3)	2.730(2)	173(3)
330 K				
O3—H31O18(−z, −x, −1 − y)	*	*	2.72(1)	*
O3—H32O52#3	*	*	2.83(1)	*
O18—H181O51#5	*	*	2.75(1)	*

^[a] At 330 K, the hydrogen atoms could not be localized. Labeled atoms are generated by the following symmetry operations: #3: −x, −, −z; #5: −y, −z, −x.

the cations are parallel to each other. They are aligned along the *a*, *b*, and *c* directions. This crystal packing is very different from the packing of [Fe₃(iptrtz)₆(H₂O)₆](tosylate)₆ · 2 H₂O (iptrtz = 4-isopropyl-1,2,4-triazole) where the adjacent entities are perpendicular to each other in one direction.^[24]

The water molecules are all coordinated to an iron(II) ion, and no free water molecules have been found in the network. This characteristic has already been observed in the structures of the trinuclear compounds [Fe₃(etrz)₆(H₂O)₆](CF₃SO₃)₆^[22] and [Fe₃(iptrtz)₆(H₂O)₆]I₆.^[29] However, this lack of supplementary water molecules does not imply the absence of a hydrogen-bonding network. Figure 2 displays a view of the intermolecular interactions at 120 K and Table 2 gives the relative bond lengths and angles.

Hydrogen-bonding through the oxygen atoms of the sulfonate groups of the triflate anions (O3...O52 #3) links the coordinated water molecules. These anions are also linked by hydrogen-bonding to the hydroxy groups of the ethyl chain in the 4-position of the triazole ligands (O18...O51 #5). The trinuclear units are not isolated. Indeed, they are linked to each other by hydrogen-bonding interactions. These are situated between the water molecules and the hydroxy groups of the triazole ligands (O3...O18; −y, −z,

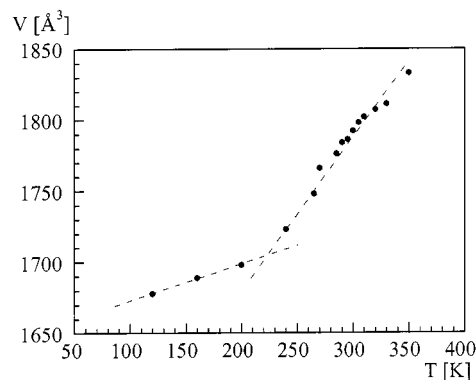


Figure 3. Temperature dependence of the cell volume of [Fe₃(hyetrz)₆(H₂O)₆](CF₃SO₃)₆

−x). The related O...O distances do not vary with temperature (Table 2).

No intramolecular interaction between different hydroxy groups of the same trinuclear unit has been detected. This situation is in contrast to the structure of the Cu^{II} linear chain compound [Cu(hyetrz)₃](ClO₄)₂ · 3 H₂O, where hydrogen bonding between hydroxy groups arising from different N1,N2–1,2,4-triazole bridges were found.^[20]

Temperature Dependence of the Cell Parameters

The symmetry of the cell is the same on both sides of the spin transition. The crystal system implies a strict isotropy of the thermal contraction. Figure 3 shows the temperature dependence of the cell volume from 120 K to 350 K. Within this range, the volume variation of 7.3% and the differential dV/VdT of 3.44 · 10^{−4} K^{−1} are comparable to the average value calculated for a series of mononuclear iron(II) spin crossover compounds (6.5% and ≈ 3.5 · 10^{−4} K^{−1}).^[30] Two different domains can be defined in this curve: a first one from 350 K to 225 K where the volume contraction (5.6%, 5.6 · 10^{−4} K^{−1}) corresponds to the contributions of the spin transition and the thermal contraction, and a second one from 225 K to 120 K where the volume decrease is only due to the thermal contraction (1.7%, 1.6 · 10^{−4} K^{−1}). In the first domain, we can roughly estimate the volume variation due to the spin transition by subtracting the contribution due to the thermal variation with the hypothesis that the behavior is the same as in the second domain. Such a value, ΔV_{SC} ≈ 90 Å³, is very similar to the volume contraction due to the spin crossover found in previously published mononuclear compounds, ΔV_{SC} ≈ 80–90 Å.^[30,31]

Magnetic Properties

The magnetic behavior of [Fe₃(hyetrz)₆(H₂O)₆](CF₃SO₃)₆ is shown in Figure 4 in the form of a χ_MT vs. T plot, χ_M being the molar magnetic susceptibility and T being the temperature. At 77 K the χ_MT value is 7.40 cm³ K mol^{−1}, which is about the value expected for two iron(II) ions in the HS state. The value of χ_MT remains constant upon heating up to 235 K, after which it increases progressively reaching a value of 10.92 cm³ K mol^{−1} at 360 K, which corresponds to the expected value for three iron(II) ions in

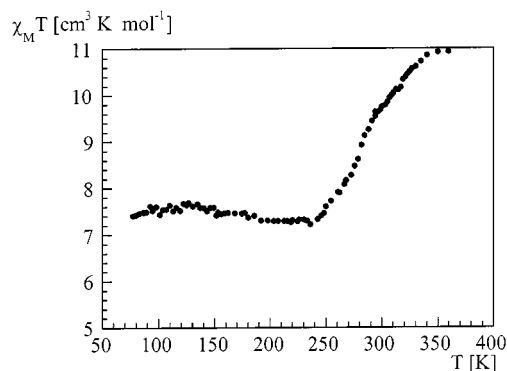


Figure 4. Evolution of $\chi_M T$ vs. T for $[\text{Fe}_3(\text{hyetrz})_6(\text{H}_2\text{O})_6](\text{CF}_3\text{SO}_3)_6$

the HS state. A similar magnetic behavior has been observed upon cooling for this gradual transition. The transition temperature $T_{1/2}$, for which 50% of the sites involved in the conversion are HS and 50% are LS, is equal to 290 K. The temperature range in which 80% of central iron(II) ions change spin state (ΔT_{80}) is 70 K. This value has to be compared with the 40 K found for $[\text{Fe}_3(\text{etrz})_6(\text{H}_2\text{O})_6](\text{CF}_3\text{SO}_3)_6$.^[22]

The assumption of negligible magnetic exchange between second-neighbor iron(II) ions is justified in view of the study of the $N1,N2$ -1,2,4-triazole triply-bridged $\text{Fe}^{\text{II}}-\text{Fe}^{\text{II}}-\text{Fe}^{\text{II}}$ ^[22] and $\text{Co}^{\text{II}}-\text{Co}^{\text{III}}-\text{Co}^{\text{II}}$ ^[32] trinuclear clusters, where the central metal ion is diamagnetic, and no magnetic interactions could be detected between the paramagnetic terminal metal ions.

Optical Measurements

Since this compound is highly thermochromic, the Fe^{II} spin transition has been studied optically using a specially designed device.^[12,13] This technique provides an accurate determination of the transition temperature although it does not give any information regarding the percentage of Fe^{II} ions involved in the spin transition. A similar ST behavior as found by magnetic measurements has been observed, with $T_{1/2} = 292$ K.

Mössbauer Measurements

^{57}Fe Mössbauer spectra were recorded at several temperatures between 4.2 K and 293 K. Parameters derived from least-squares fitting are listed in Table 3.

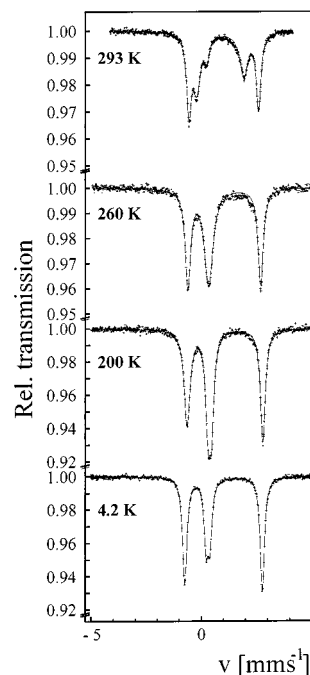


Figure 5. Selected ^{57}Fe Mössbauer spectra of $[\text{Fe}_3(\text{hyetrz})_6(\text{H}_2\text{O})_6](\text{CF}_3\text{SO}_3)_6$ recorded at different temperatures

As can be seen from Figure 5, the spectrum measured at 4.2 K shows the expected structure for a trinuclear iron(II) 1,2,4-triazole compound with two iron(II) ions in the HS state and one in the LS state with a relative intensity 1:2. The outer two lines refer to the quadrupole doublet arising from the two peripheral iron(II) ions in the HS state. The signal in the middle represents the poorly resolved quadrupole doublet of the central iron(II) ion in the LS state. The small splitting of the LS doublet indicates that the local environment of the central iron(II) ion is not symmetric, which is not seen in the crystal structure at 120 K. On heating the sample up to 200 K, the spectrum remains essentially the same, with the difference observed between the intensities of the LS and HS doublets being attributed to the known difference of the Debye–Waller factors for the two species. The Debye–Waller factor for the LS state is generally larger (by ca. 20%) than that for the HS state and shows a different temperature dependence for the two states. The consequence of this situation is that the area fractions of the Mössbauer resonance lines do not reflect exactly the actual concentrations of the two states; the LS

Table 3. ^{57}Fe Mössbauer parameters of $[\text{Fe}_3(\text{hyetrz})_6(\text{H}_2\text{O})_6](\text{CF}_3\text{SO}_3)_6$

T [K]	δ [mm s ⁻¹]	ΔE_Q [mm s ⁻¹]	Γ [mm s ⁻¹]	rel. area [%]	Spin state
4.2 ^[a]	0.301 ± 0.001	0.172 ± 0.002	0.125 ± 0.004	34.5 ± 0.7	LS
	1.007 ± 0.001	3.510 ± 0.001	0.132 ± 0.002	65.5 ± 0.4	HS
200	0.383 ± 0.007	0.162 ± 0.004	0.182 ± 0.003	45.5 ± 1.3	LS
	1.071 ± 0.001	3.426 ± 0.003	0.144 ± 0.003	54.5 ± 1.8	HS
260	0.331 ± 0.004	—	0.234 ± 0.013	45.0 ± 1.9	LS
	1.039 ± 0.002	3.289 ± 0.004	0.145 ± 0.003	55.0 ± 2.1	HS
293	0.253 ± 0.008	—	0.128 ± 0.014	24.2 ± 1.2	LS
	1.016 ± 0.002	3.152 ± 0.003	0.123 ± 0.003	47.7 ± 3.5	HS
	0.858 ± 0.004	2.133 ± 0.008	0.226 ± 0.007	28.0 ± 2.3	HS

^[a] The temperature of the $^{57}\text{Co}(\text{Rh})$ source was 4.2 K.

state rather is overestimated due to the higher tightness of binding in the LS iron complex molecules as compared to the HS complex molecules. At 260 K, the HS doublet attributed to the external iron(II) ions remains the same but the HS doublet of the central iron(II) ion is not distinguishable while the spin crossover occurs at this temperature (cf. Figure 3 and Figure 4). An unusual broadening of the lines of the LS doublet is observed, which is most likely due to the dynamic nature of the spin crossover behavior. At room temperature the spectrum shows two additional lines attributed to the LS and HS species of the central iron(II) ion with an approximate intensity ratio of 1:1, indicating that the transition temperature $T_{1/2}$ is near to 290 K [the peak in the middle refers to the LS state of the central iron(II) ion, the two neighboring signals constitute the HS quadrupole doublet of the central iron(II) ion, and the outer two signals are the quadrupole doublet of the two peripheral iron(II) ions]. Because the relaxation phenomenon is still present at room temperature, the lines of the new HS species together with the remainder of the LS species are about twice as broad as the lines of the external Fe^{II} ions. In the present study, we have restricted ourselves to a qualitative approach to the relaxation phenomenon. For a quantitative analysis, the ⁵⁷Fe Mössbauer relaxation spectra in the spin crossover region should be fitted using the corresponding relaxation theory,^[33] which is a very elaborate task and is beyond the scope of this study. At room temperature, one notices that the isomer shift and the quadrupole splitting of the central and the peripheral iron(II) ions in the HS state do not coincide (see Table 3). This is clear from the fact that the first coordination spheres are different, namely the presence of only nitrogen atoms for the central iron(II) ion and mixed nitrogen-oxygen surroundings for peripheral iron(II) ions. This, of course, gives rise to different electric field gradients and thus different electric quadrupole interactions for the two inequivalent iron sites.

The Mössbauer experiment at 4.2 K was also carried out in an external magnetic field of 5 T directed parallel to the γ -ray beam. The obtained spectrum (Figure 6) exhibits two groups of sextets with the following hyperfine parameters:

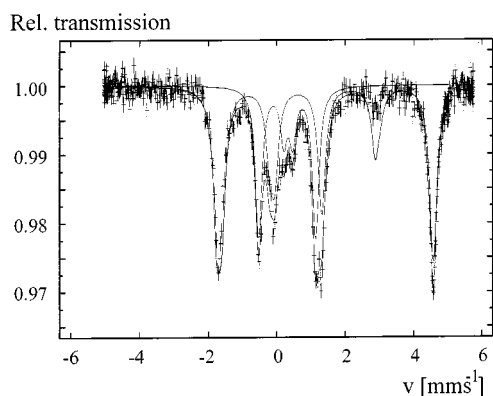


Figure 6. ⁵⁷Fe Mössbauer spectrum of [Fe₃(hyetrz)₆(H₂O)₆](CF₃SO₃)₆ recorded at 4.2 K in an external magnetic field of 5 T parallel to the direction of the γ rays

$H_{LS} = 5.16$ T, $\delta_{LS} = 0.307$ mm s⁻¹, $\Delta EQ_{LS} = -0.03 \pm 0.01$ mm s⁻¹, $\phi_{LS} = 0^\circ$; $H_{HS} = 13.1$ T, $\delta_{HS} = 1.004$ mm s⁻¹, $\Delta EQ_{HS} = -3.51 \pm 0.01$ mm s⁻¹, $\phi_{HS} = 87.3^\circ$. ϕ_{LS} and ϕ_{HS} characterize the polar angles between the principal axis V_{ZZ} of the electrical field gradient and the local magnetic field H at the iron nuclei of LS and HS states. Analyzing the values of the hyperfine parameters, one can conclude the following. Negative signs of the quadrupole splitting on both states indicate that the orbital singlet is the ground state. This means that the three octahedra are elongated along the trigonal axes of the trinuclear unit. This conclusion is in agreement with the structural data obtained at 120 K. In the LS state the iron nuclei only “see” the external magnetic field. Because of the spatial averaging for the powder sample the effective value of the polar angle ϕ_{LS} is zero. In the HS state, the external magnetic field induces slow spin-lattice relaxation and the effective field on the iron nuclei is a superposition of both external and internal fields. The internal magnetic field is nearly perpendicular to the direction of V_{ZZ} ($\phi_{HS} = 87.3^\circ$), which apparently coincides with the axial axis of the trinuclear unit. It is noteworthy that the deviation of the magnetic field axis from the nearly perpendicular V_{zz} axis almost coincides with the deviation of 3° found between the parts containing oxygen and nitrogen atoms of the peripheral irregular octahedra of the trinuclear unit.

Discussion and Conclusion

In this paper we have described the molecular structure as well as the magnetic properties of a new linear trinuclear iron(II) spin crossover compound. The spin transition regime is centered in the room temperature region. The crystal structure has been solved above and below the transition temperature. If we compare the hyetrz ligand with its homolog, the etrz ligand, the chain in the 4-position of the 1,2,4-triazole has been functionalized by the introduction of a hydroxy group. This substituent has been selected for its potential to be linked by hydrogen bonding interactions to other entities of the network. Therefore, we can expect an increase in the intermolecular interactions in comparison to the trinuclear compound formed with the etrz ligand, [Fe₃(etrz)₆(H₂O)₆](CF₃SO₃)₆.^[22] This has been borne out experimentally, because a molecular assembly of linear trinuclear entities linked by an unprecedented three-dimensional network of hydrogen bonds has been discovered for the title compound. The hydroxy groups play the role of bridges between the trinuclear units by hydrogen bonding with the water molecules coordinated to metal ions. Besides, the triflate anions allow the strengthening of the interactions, by hydrogen bonding with the water molecules and the alcohol groups.

Regarding the magnetic properties, a weak cooperative spin crossover behavior was observed. This can be understood if one considers the isolated molecule where only the central metal ion undergoes the spin crossover. However, surprisingly, the ST curve of this material is less abrupt than

the one found for $[\text{Fe}_3(\text{etrz})_6(\text{H}_2\text{O})_6](\text{CF}_3\text{SO}_3)_6$, as given by the comparison of the ΔT_{80} values for these two compounds. This could indicate that the presence of intermolecular interactions by hydrogen bonding would not have a favorable effect on the cooperativity developed by such trinuclear systems. A loss of cooperativity in this way has already been observed for the linear trinuclear compounds $[\text{Fe}_3(\text{iptrz})_6(\text{H}_2\text{O})_6](\text{CF}_3\text{SO}_3)_6$ and $[\text{Fe}_3(\text{iptrz})_6(\text{H}_2\text{O})_6](\text{tosylate})_6 \cdot 2 \text{H}_2\text{O}$.^[24] The tosylate derivative, which presents a less cooperative spin crossover behavior, shows a crystal structure in which the trinuclear units are linked to the anions and the noncoordinated water molecules by hydrogen bonding. This network, assumed to be more flexible than the one found for the triflate derivative (which does not include any lattice water molecules) was taken as being responsible for the less cooperative behavior of the observed transition. This hypothesis could also be valid for $[\text{Fe}_3(\text{hyetrz})_6(\text{H}_2\text{O})_6](\text{CF}_3\text{SO}_3)_6$. It is interesting to note that the transition temperature, which is 203 K for $[\text{Fe}_3(\text{etrz})_6(\text{H}_2\text{O})_6](\text{CF}_3\text{SO}_3)_6$, is now 290 K for the title compound. Thus, a pronounced shift of $T_{1/2}$ towards higher temperatures has been observed. This behavior can be directly attributed to the introduction of hydrogen bonds into the network, a property that apparently increases the ligand field strength at the central iron ion. This stabilization of the LS state by hydrogen bonding has already been reported for other ST compounds; for instance the case for the Fe^{II} linear chain compound $[\text{Fe}(\text{hyetrz})_3](3\text{-nitrophenylsulfonate})_2$.^[14,17] The dehydrated material shows a spin crossover behavior at low temperature whereas the hydrated material is LS at room temperature. Thus, in this case, the inclusion of water molecules through hydrogen bonding stabilizes the LS state. Such an effect has also been observed in the mononuclear spin crossover complex $[\text{Fe}(\text{2-pic})_3]\text{Cl}_2 \cdot \text{Sol}$ with 2-pic = 2-picolyamine, where the system with Sol = H_2O still exhibits thermal spin crossover although with a very large hysteresis, but the system with Sol = $2 \cdot \text{H}_2\text{O}$ shows LS behavior up to room temperature.^[34]

Pronounced relaxation effects have been evidenced by ^{57}Fe Mössbauer spectroscopy for $[\text{Fe}_3(\text{hyetrz})_6(\text{H}_2\text{O})_6](\text{CF}_3\text{SO}_3)_6$ by virtue of considerable resonance line broadening. Clear evidence of the dynamic nature of the spin crossover behavior was revealed from the very beginning of the spin transition (260 K). This is in contrast with $[\text{Fe}(\text{2-pic})_3](\text{PF}_6)_2$ ($T_{1/2} = 178.5 \text{ K}$) where relaxation effects were only found below 200 K, which is near to the completion of the spin transition.^[33] In addition, intersystem crossing dynamics in the solid state for this mononuclear compound were found to be very similar to other Fe^{II} compounds in solution. In the case of trinuclear compounds, the analogy with liquids is much more reasonable because the spin crossover entities are more isolated from each other in comparison to mononuclear compounds. In this case we are dealing with a diluted system. For this reason one could consider trinuclear systems as good candidates for the study of the dynamics of the spin crossover interconversion in the solid state. To the best of our knowledge, the title compound is the first to exhibit such pronounced features of relaxation in the solid state.^{[33,35]–[39]} This is probably related to its very high transition temperature,^[37] or to the simultaneous onset of molecular motions and spin crossover behavior. In other words, these two latter processes may be interconnected. Having learned that Fe^{II} trinuclear compounds could exhibit relaxation effects, we cannot exclude that this could also be responsible for the broadening of the lines of the LS doublet at 242 K for $[\text{Fe}_3(\text{iptrz})_6(\text{H}_2\text{O})_6](\text{tosylate})_6$ with iptrz = 4-isopropyl-1,2,4-triazole.^[24] This effect could also be present for other Fe^{II} spin crossover compounds like, for example, $[\text{Fe}\{\text{HB}(\text{trz})_3\}_2]$ with $\text{HB}(\text{trz})_3 = \text{hydrotris}(1,2,4\text{-triazolyl})\text{borate}$.^[40]

Mössbauer experiments performed in the presence of an external magnetic field could allow us to confirm the structural data. This technique could, in future, provide structural information for other Fe^{II} trinuclear compounds for which the crystal structure is not yet available.^[23,24] We intend to revisit this aspect in a subsequent paper.

Table 4. Crystallographic data of $[\text{Fe}_3(\text{hyetrz})_6(\text{H}_2\text{O})_6](\text{CF}_3\text{SO}_3)_6$ at 120 K and 330 K

	$\text{C}_{30}\text{H}_{54}\text{F}_{18}\text{Fe}_3\text{N}_{18}\text{O}_{30}\text{S}_6$	$\text{C}_{30}\text{H}_{54}\text{F}_{18}\text{Fe}_3\text{N}_{18}\text{O}_{30}\text{S}_6$
Formula	$\text{C}_{30}\text{H}_{54}\text{F}_{18}\text{Fe}_3\text{N}_{18}\text{O}_{30}\text{S}_6$	$\text{C}_{30}\text{H}_{54}\text{F}_{18}\text{Fe}_3\text{N}_{18}\text{O}_{30}\text{S}_6$
Molecular weight	1848.52	1848.52
T [K]	120	330
Color	purple	colorless
Dimensions [mm ³]	$0.5 \times 0.25 \times 0.25$	$1.6 \times 0.80 \times 0.80$
Space group	$R\bar{3}$ (no. 148)	$R\bar{3}$ (no. 148)
a, b, c [Å]	12.7363(1)	13.0183(3)
α, β, γ [°]	67.144(1)	67.376(3)
V [Å ³]	1684.3(1)	1805.8(1)
Z	1	1
$\rho_{\text{calcd.}}$ [g cm ⁻³]	1.82	1.70
Device	SMART CCD	SMART CCD
λ [Å], Mo- K_{α}	0.71073	0.71073
μ [cm ⁻¹]	9.68	9.02
Collected Reflections	18135	4608
Obs. Uniq. Reflections	2586	1976
R_{int}	0.019	0.049
Parameters	195	165
$R(F)^{[\text{a}]}$	0.022	0.063
$wR(F)^2$ [a]	0.056	0.174
S	1.07	1.04

[a] $R(F) = \Sigma \|F_o\| - |F_c| / \Sigma |F_o|$ for $F_o > 4\sigma(F_o)$, $wR(F)^2 = [\Sigma w(F_o^2 - F_c^2)^2 / \Sigma wF_o^2]^{1/2}$, $w = 1/(\sigma^2(F_o^2) + 0.035F^2)$; $S = (\Sigma_i w_i \Delta\Phi^2)/(n - m)$.

Experimental Section

Starting Materials: Commercially available solvents, monoformyl hydrazine, triethylorthoformate, 2-ethanolamine, and iron(II) triflate were used without further purification.

Synthesis of [Fe₃(hyetrz)₆(H₂O)₆](CF₃SO₃)₆: The ligand 4-(2'-hydroxyethyl)-1,2,4-triazole (hyetrz) was prepared as described previously.^[20] A solution of hyetrz (1.06 mmol, 0.12 g) in water (10 mL) was added to a solution of Fe(CF₃SO₃)₂ · 6 H₂O (0.54 mmol, 0.25 g) in water (20 mL). The volume of the solution was reduced to 15 mL. After two weeks, the mauve compound crystallized upon slow evaporation of the colorless solution at room temperature. The crystals were filtered off, washed with water and dried under ambient air. Yield: 17%. IR: $\tilde{\nu}_{\text{am}}(\text{SO}_3^-) = 1279 \text{ cm}^{-1}$.

Physical Measurements: Magnetic susceptibilities were measured in the temperature range 77–400 K with a fully automated Manics DSM-8 susceptometer equipped with an Oxford instruments DN170 continuous-flow cryostat and a Bruker BE15f electromagnet operating at ca. 0.8 Tesla. Data were corrected for magnetization of the sample holder and for diamagnetic contributions, which were estimated from the Pascal constants. — Optical measurements were carried out using the device described previously^[12,13] with a heating rate of 1 K min⁻¹ in the temperature range 77–400 K. Mössbauer spectra were recorded in transmission geometry with a Co/Rh source kept at liquid helium temperature and a conventional spectrometer operating in the constant-acceleration mode. The samples were sealed in a Plexiglass sample holder and mounted in a helium-bath cryostat. The cryostat was equipped with a superconductor solenoid operating with a field of 5 T. The spectra were fitted to Lorentzian-shaped lines using a nonlinear iterative minimization routine (MOSFUN).

Crystallographic Data Collection and Structure Determination: Experimental and crystal data are reported in Table 4. The single crystals appear pink at 293 K and purple at 120 K. This color is due to the ¹A_{1g} → ¹T_{1g} d-d transition of LS Fe^{II} occurring at 520 nm. The color of the compound changes to colorless upon heating to ca. 330 K. This is due to the fact that the spin-allowed d-d transition of lowest energy of the compound in the HS state, ⁵T_{2g} → ⁵E_g, occurs at the limit of the visible and IR regions. The structural properties have been investigated from 120 K to 330 K with a Bruker Smart diffractometer associated with an Oxford Cryo-System nitrogen open cryostat. A first sample was cooled to 120 K at a rate of 2 K min⁻¹. 3024 frames were collected using ω scans in 0.2° steps with a 10 s time exposure per frame. Complete data collection was also performed at 293 K and at 310 K but no coherent data could be obtained and the structure could not be solved. A second crystal was used to collect the data at 330 K where the spin crossover is almost complete. Unfortunately, the single crystals melt at this temperature after around four hours, which did not allow us to finish the data collection. The same strategy of data collection as at 120 K was used but only the first 770 frames could be used, which nevertheless gave enough unique observed reflections (1976 observed reflections for 165 refined parameters). Finally, a third crystal was used to determine the cell parameter evolution from 120 K to 330 K. The computing data reduction was performed using the SAINT package including absorption correction using the SADABS program.^[41] Such a correction slightly improved the internal R factor (decrease of 1.5%). The crystal structures were solved and refined with SHELXTL.^[42] The full-matrix least square refinement of the atomic parameters was based on F². All the non-hydrogen atoms were refined with anisotropic thermal parameters.

The crystal structure at 330 K is clearly not very accurate, mainly due to the very large thermal motion. Hydrogen atoms were placed using difference Fourier maps at 120 K and their atomic positions were refined, while it was not possible to locate them at 330 K.

Crystallographic data have been deposited at the Cambridge Crystallographic Data Centre as supplementary publication no CCDC-134366 for the structure at 330 K and CCDC-134367 for the structure at 120 K. Copies of the data can be obtained free of charge on application to CCDC, 12 Union Road, Cambridge CB21EZ, UK [Fax: (+44) 1223/336-033; E-mail: deposit@ccdc.cam.ac.uk].

Acknowledgments

This work was partly funded by the TMR Research Network ERB-FMRX-CT98-0199 entitled "Thermal and Optical Switching of Molecular Spin States (TOSS)". P. G. and Y. G. also express their thanks to the Fonds der Chemischen Industrie and the Materialwissenschaftliches Forschungszentrum der Universität Mainz for financial support.

- [1] O. Kahn, J. P. Launay, *Chemtronics* **1988**, 3, 140.
- [2] J. Zarembowitch, O. Kahn, *New. J. Chem.* **1991**, 15, 181.
- [3] O. Kahn, *Molecular Magnetism*, VCH, New York, **1993**.
- [4] H. A. Goodwin, *Coord. Chem. Rev.* **1976**, 18, 293.
- [5] P. Gülich, *Struct. Bonding (Berlin)* **1981**, 44, 83.
- [6] P. Gülich, A. Hauser, H. Spiering, *Angew. Chem. Int. Ed. Engl.* **1994**, 33, 2024 and references therein.
- [7] [7a] P. Gülich, J. Jung, *J. Mol. Struct.* **1995**, 347, 21. — [7b] P. Gülich, J. Jung, H. A. Goodwin, *NATO ASI Series C*, Kluwer, Dordrecht, The Netherlands, **1996**, p. 327. — [7c] P. Gülich, J. Jung, *Nuovo Cimento Soc. Ital. Fis. D* **1996**, 18, 107. — [7d] P. Gülich, *Mol. Cryst. Liq. Cryst.* **1997**, 305, 17. — [7e] P. Gülich, H. Spiering, A. Hauser, in: *Inorganic Electronic Structure and Spectroscopy* (Eds.: E. I. Solomon, A. B. P. Lever), John Wiley & Sons, Inc., **1999**, p. 575.
- [8] [8a] O. Kahn, E. Codjovi, Y. Garcia, P. J. van Koningsbruggen, R. Lapouyade, L. Sommier, *Symp. Ser.* **1996**, 644, 298. — [8b] O. Kahn, C. Jay-Martinez, *Science* **1998**, 279, 44. — [8c] O. Kahn, Y. Garcia, J. F. Letard, C. Mathonière, NATO ASI Series, Kluwer, Dordrecht, The Netherlands, **1998**, p. 127.
- [9] O. Kahn, J. Kröber, C. Jay, *Adv. Mater.* **1992**, 4, 718.
- [10] J. Kröber, E. Codjovi, O. Kahn, F. Grolière, C. Jay, *J. Am. Chem. Soc.* **1993**, 115, 9810.
- [11] J. Kröber, J. P. Audié, R. Claude, E. Codjovi, O. Kahn, J. G. Haasnoot, F. Grolière, C. Jay, A. Bousseksou, J. Linares, F. Varret, A. Gonthier-Vassal, *Chem. Mater.* **1994**, 6, 1404.
- [12] O. Kahn, E. Codjovi, *Phil. Trans. R. Soc. London* **1996**, A354, 359.
- [13] E. Codjovi, L. Sommier, O. Kahn, C. Jay, *New J. Chem.* **1996**, 20, 503.
- [14] Y. Garcia, P. J. van Koningsbruggen, E. Codjovi, R. Lapouyade, O. Kahn, L. Rabardel, *J. Mater. Chem.* **1997**, 7, 857.
- [15] P. J. van Koningsbruggen, Y. Garcia, E. Codjovi, R. Lapouyade, O. Kahn, L. Fournès, L. Rabardel, *J. Mater. Chem.* **1997**, 7, 2069.
- [16] Y. Garcia, P. J. van Koningsbruggen, R. Lapouyade, L. Rabardel, O. Kahn, M. Wierczorek, R. Bronisz, Z. Ciunik, M. F. Rudolf, *C. R. Acad. Sci. Paris* **1998**, IIc, 523.
- [17] Y. Garcia, P. J. van Koningsbruggen, R. Lapouyade, L. Fournès, L. Rabardel, O. Kahn, V. Ksenofontov, G. Levchenko, P. Gülich, *Chem. Mater.* **1998**, 10, 2426.
- [18] C. Jay, F. Grolière, O. Kahn, J. Kröber, *Mol. Cryst. Liq. Cryst.* **1993**, 234, 255.
- [19] V. P. Sinditskii, V. I. Sokol, A. E. Fogel'zang, M. D. Dutov, V. V. Serushkin, M. A. Porai-Koshits, B. S. Svetlov, *Russ. J. Inorg. Chem.* **1987**, 32, 1149.
- [20] Y. Garcia, P. J. van Koningsbruggen, G. Bravic, P. Guionneau, D. Chasseau, G. L. Cascarano, J. Moscovici, K. Lambert, A. Michalowicz, O. Kahn, *Inorg. Chem.* **1997**, 36, 6357.
- [21] Y. Garcia, Ph.D. thesis, University of Bordeaux I (France), **1999**.

- [22] [22a] G. Vos, R. A. Le Fèvre, R. A. G. de Graaff, J. G. Haasnoot, J. Reedijk, *J. Am. Chem. Soc.* **1983**, *105*, 1682. — [22b] G. Vos, R. A. G. de Graaff, J. G. Haasnoot, A. M. van der Kraan, P. de Vaal, J. Reedijk, *Inorg. Chem.* **1984**, *23*, 2905.
- [23] M. Thomann, O. Kahn, J. Guilhem, F. Varret, *Inorg. Chem.* **1994**, *33*, 6029.
- [24] J. J. A. Kolnaar, G. van Dijk, H. Kooijman, A. L. Spek, V. G. Ksenofontov, P. Gütllich, J. G. Haasnoot, J. Reedijk, *Inorg. Chem.* **1997**, *36*, 2433.
- [25] A. Michalowicz, J. Moscovici, B. Ducourant, D. Cracco, O. Kahn, *Chem. Mater.* **1995**, *7*, 1833.
- [26] E. König, *Prog. Inorg. Chem.* **1987**, *35*, 527.
- [27] A. L. Spek, G. Vos, *Acta Cryst.* **1983**, *C39*, 990.
- [28] G. Vos, J. G. Haasnoot, G. C. Verschoor, J. Reedijk, P. E. L. Schaminee, *Inorg. Chim. Acta* **1985**, *105*, 31.
- [29] J. J. A. Kolnaar, Ph.D. Thesis, University of Leiden, **1998**.
- [30] P. Guionneau, J. F. Létard, D. S. Yuffit, D. Chasseau, J. A. K. Howard, A. E. Goeta, O. Kahn, *J. Mater. Chem.* **1999**, *4*, 985.
- [31] M. Mikami, M. Konno, Y. Saito, *Chem. Phys. Lett.* **1979**, *63*, 566.
- [32] L. Antolini, A. C. Fabretti, D. Gatteschi, A. Giusti, R. Sessoli, *Inorg. Chem.* **1991**, *30*, 4858.
- [33] P. Adler, H. Spiering, P. Gütllich, *Inorg. Chem.* **1987**, *26*, 3840.
- [34] M. Sorai, J. Ensling, K. M. Hasselbach, P. Gütllich, *Chem. Phys.* **1977**, *20*, 197.
- [35] H. R. Chang, J. K. McCusker, H. Toftlund, S. R. Wilson, A. X. Trautwein, H. Winkler, D. N. Hendrickson, *J. Am. Chem. Soc.* **1990**, *112*, 6814.
- [36] E. König, *Struct. Bonding (Berlin)* **1991**, *76*, 51.
- [37] A. Bousseksou, C. Place, J. Linares, F. Varret, *J. Magn. Magn. Mat.* **1992**, *104*, 225.
- [38] G. Lemerrier, A. Bousseksou, M. Verelst, F. Varret, J. P. Tuchagues, *J. Magn. Magn. Mat.* **1995**, *150*, 227.
- [39] P. J. Kunkeler, P. J. van Koningsbruggen, J. P. Cornelissen, A. M. van der Horst, A. M. van der Kraan, A. L. Spek, J. G. Haasnoot, J. Reedijk, *J. Am. Chem. Soc.* **1996**, *118*, 2190.
- [40] C. Janiak, T. G. Scharmann, J. C. Green, R. P. G. Parkin, M. J. Kolm, E. Riedel, W. Mickler, J. Elguero, R. M. Claramunt, D. Sanz, *Chem. Eur. J.* **1996**, *2*, 992.
- [41] *SMART Version 4.050*. Siemens Analytical X-ray Instruments, Madison WI, U.S.A., **1995**.
- [42] G. M. Sheldrick, *SHELXTL-Plus. Release 4.1*. Siemens Analytical X-ray Instruments Inc., Madison WI, U.S.A., **1991**.

Received November 24, 1999
[199424]